Molecular Crystals and Liquid Crystals
Publication details, including instructions for authors and subscription information:
http://www.tandfonline.com/loi/gmcl20

Dielectric and Optical Behavior of Two Calamitic Hydrogen-Bonded Mesogens

R. Manohar [a], Deepa Pal [a], Shashwati [b], V. S. Chandel [c], Z. U. Mazumdar [d], M. K. Paul [d] & N. V. S. Rao [d]

[a] Department of Physics, University of Lucknow, Lucknow, India
[b] Department of Physics, R M L Awadh University, Faizabad, India
[c] Department of Physics, Integral University, Lucknow, India
[d] Department of Chemistry, Assam University, Silchar, India

Available online: 27 Dec 2011

To cite this article: R. Manohar, Deepa Pal, Shashwati, V. S. Chandel, Z. U. Mazumdar, M. K. Paul & N. V. S. Rao (2012): Dielectric and Optical Behavior of Two Calamitic Hydrogen-Bonded Mesogens, Molecular Crystals and Liquid Crystals, 552:1, 71-82

To link to this article: http://dx.doi.org/10.1080/15421406.2011.604267

Mol. Cryst. Liq. Cryst., Vol. 552: pp. 71–82, 2012

ISSN: 1542-1406 print/1563-5287 online
DOI: 10.1080/15421406.2011.604267

Taylor & Francis
Taylor & Francis Group

Dielectric and Optical Behavior of Two Calamitic Hydrogen-Bonded Mesogens

R. MANOHAR,[1,*] DEEPA PAL,[1] SHASHWATI,[2]
V. S. CHANDEL,[3] Z. U. MAZUMDAR,[4] M. K. PAUL,[4]
AND N. V. S. RAO[4]

[1]Department of Physics, University of Lucknow, Lucknow, India
[2]Department of Physics, R M L Awadh University, Faizabad, India
[3]Department of Physics, Integral University, Lucknow, India
[4]Department of Chemistry, Assam University, Silchar, India

Temperature variation of dielectric loss, dielectric permittivity and percentage optical transmittance of two calamitic H-bonded mesogens $C_4P_y12B\bar{a}$ and $C_4P_y10B\bar{a}$ have been reported in the temperature range of 80°C to 140°C. The dielectric loss and dielectric permittivity have also been measured with variation of frequency. The dielectric studies have been conducted in the frequency range of 1 kHz to 5 MHz. Transition temperatures obtained by using different techniques are found to be in good agreement with each other.

Keywords Dielectric properties; H-bonded mesogens; optical properties; phase transitions

PACS No. 78.20.Ci; 77.84.N

1. Introduction

The formation of molecular aggregates is greatly dependent upon intermolecular interactions [1]. The molecular aggregates lead to supramolecular molecular structures. The self-assembly and self-organization of supramolecular molecular aggregates leads to liquid crystal behavior. The application of H-bonding in the formation of novel liquid crystalline materials, that is, supramolecular mesogens has been rapidly developed in the last three decades after the discovery of hydrogen bonded liquid crystals by Kato and Frechet in 1989 [2]. Supramolecular mesogens are molecular complexes generated from complexation of molecular species through non-covalent interactions, that is, hydrogen bonding. A significant number of new structures can be realized by a proper combination of different proton donors and proton acceptors, which are different from their original moieties to yield different liquid crystalline variants [3]. The chemistry and physics of the H-bonded mesogens have recently been discussed in several review articles [3–6]. The ease of tailoring and modification of the supramolecular structures, H-bonded mesogenic materials offers a wide variety of unusual molecular shapes and allow a large range of potential applications in the diverse fields of electro optical display devices and gels. These Liquid crystalline materials

*Address correspondence to R. Manohar, Department of Physics, University of Lucknow, Lucknow-226007, India. E-mail: rajiv.manohar@gmail.com

containing H-bonding between two organic molecular skeletons exhibit properties different from both the organic ligands and also offers a large polarizable electron density, which may give rise to new types of macroscopic (e.g., dielectric and optical) properties.

Dielectric spectroscopy is an important tool to investigate the static and dynamic properties of the mesogens. With the help of dielectric spectroscopy, one can easily obtain the complex dielectric permittivity of H-bonded supramolecular mesogens. It is now very easy to obtain dielectric parameter accurately with the variation of wide frequency and temperature range using computer controlled bridges and precise temperature controllers. The measurement of the transition temperatures by optical transmittance technique is one of the simple, accurate, and precise methods to obtain the transition temperatures of the liquid crystals. In this paper, the properties under investigation are the dielectric constant, dielectric loss, and optical transmittance for two hydrogen bonded mesogens samples namely $C_4P_Y10B\bar{a}$ and $C_4P_Y12B\bar{a}$.

The phase transition temperatures for both the samples are fully supported by the data obtained using the earlier two techniques.

2. Experimental Details

In the present paper, we have focused our studies on two calamitic mesogens $C_4P_Y10B\bar{a}$ and $C_4P_Y12B\bar{a}$. The structure and Differential Scanning Calorimatory (DSC) thermograms are given in Fig. 1.

The 4-*n*-decyloxybenzoic acid **10OBA**, exhibits four enantiotropic phases of smectic G, smectic C phase, cybotactic nematic, and nematic phases between 86.5°C to 141.6°C in the heating and 77.4°C to 140.5°C in the cooling cycles. The two types of nematic phases are reported, but experimentally, it is not easy to observe by differential scanning calorimetry. Thermal microscopy could not detect the phase transition. The transition between normal nematic and cybotactic nematic phase is associated with the percentage of monomer concentration. The self-hydrogen bonding of the acid dimer units decreases with increasing temperature and monomer concentration increases with the increasing temperature. The binary complex that was obtained exhibited stable liquid crystalline phases, which was confirmed by differential scanning calorimetry and thermal microscopy after repeated thermal cycles. The complex exhibited three transitions in the heating cycle at 83.1°C ($\Delta H = 7.57$ kJ mol^{-1}, $\Delta S = 21.25$ J K^{-1} mol^{-1}), 95.8°C ($\Delta H = 34.10$ kJ mol^{-1}, $\Delta S = 92.46$ J K^{-1} mol^{-1}), and 117.4°C ($\Delta H = 2.46$ kJ mol^{-1}, $\Delta S = 6.30$ J K^{-1} mol^{-1}). In the cooling cycle also, it exhibited two transitions at 116.8°C, ($\Delta H = 1.11$ kJ mol^{-1}, $\Delta S = 2.85$ J K^{-1} mol^{-1}), and 94.3°C ($\Delta H = 0.06$ kJ mol^{-1}, $\Delta S = 0.16$ J K^{-1} mol^{-1}). The nematic isotropic phase transition occurs at 117.4°C in the heating cycle Fig. 1(a).

12OBA-4PyA:

The 4-*n*-dodecyloxybenzoicacid **12OBA**, exhibits 37.2°C smectic C phase, and 6.3°C nematic phase between 95.2°C and 138.7°C. Both the molecules **12OBA** and **4PyA** are linear and possess the appropriate molecular structure to form a hydrogen bonded complex with an overall molecular geometry directed along the long axis of the individual rod like molecules. In particular, the lone pair of electrons of the pyridyl group of **4PyA** is directed along the molecular axis of the participating atoms of hydrogen bonding. In order to break the self hydrogen bonding of the acid dimer units, the equimolar components were dissolved separately in pyridine, mixed together and the solvent was slowly evaporated to obtain the complex. The binary complex that was obtained exhibited stable liquid crystalline phases, which was confirmed by differential scanning calorimetry and thermal microscopy after

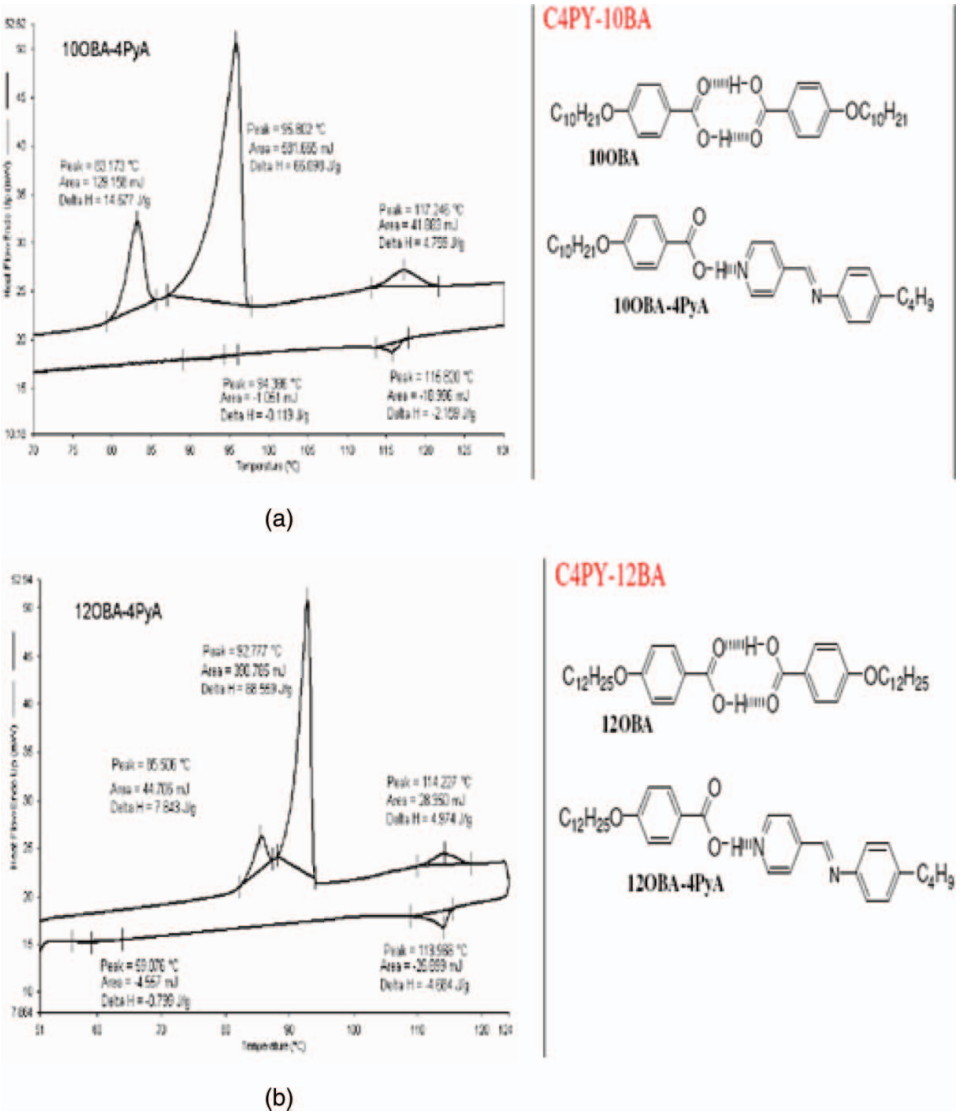

Figure 1. The structure and DSC thermograms of the samples (Color figure available online).

repeated thermal cycles. The complex exhibited three transitions in the heating cycle at 85.5°C ($\Delta H = 4.27$ kJ mol^{-1}, $\Delta S = 11.91$ J K^{-1} mol^{-1}), 92.7°C ($\Delta H = 37.29$ kJ mol^{-1}, $\Delta S = 101.97$ J K^{-1} mol^{-1}), and 114.2°C ($\Delta H = 2.71$ kJ mol^{-1}, $\Delta S = 6.99$ J K^{-1} mol^{-1}). In the cooling cycle also, it exhibited two transitions at 113.9°C ($\Delta H = 2.55$ kJ mol^{-1}, $\Delta S = 6.59$ J K^{-1} mol^{-1}), and 59.0°C ($\Delta H = 0.43$ kJ mol^{-1}, $\Delta S = 1.29$ J K^{-1} mol^{-1}). The crystallization peak did not appear and it may be due to glassy phase that may appear in higher homologues. The nematic-isotropic phase transition occurs at 127.6°C in the heating cycle Fig. 1(b).

The dielectric measurements have been performed with a computer controlled Impedance/Gain Phase Analyzer Hewlett/Packard (Model No. HP4194A). The transparent and highly conducting ITO coated optically flat glass substrate were used as electrode,

which allows one to control the optical alignment of the liquid crystal molecules and also to study the dielectric dispersion process. Both the electrodes of the cells were treated with adhesion promoter and polymer (Nylon 6/6) and rubbed unidirectionally to get the planar alignment. Thickness of the cell was maintained at 5 μm by means of a Mylar spacer. The cell was well calibrated using standard materials, CCl_4 and benzene. The liquid crystal material was introduced into the cell by mean of a capillary action at its isotropic temperature. A well aligned cell was obtained by applying an electric field in the slow cooling cycle from the isotropic to room temperature and simultaneously observing it under polarizing microscope (CENSICO 7626). Instec hot plate (HCS302) is used for required temperature stability providing an accuracy of $\pm$ 0.1°C.

The values of capacitance and conductance of the sample holder with and without sample has been measured using a gain phase analyzer. The real and imaginary part of permittivity of the sample has been obtained, using the equations (1) and (2) [7, 8].

$$\varepsilon' = \frac{C_m - C_O}{C_l} + 1 \tag{1}$$

and

$$\varepsilon'' = \frac{(G_m - G_o)}{2\pi f C_l} \tag{2}$$

where C_m and G_m are the capacitance and conductance of cell filled with sample, C_o and G_o are the capacitance and conductance of cell without sample and C_l is the live capacitance.

The capacitance values were read up to three places of decimal while dissipation factor were recorded up to fourth place of decimal in the frequency range of 1 kHz to 10 MHz. For the optical transmittance measurement, sample holder filled with sample has been placed between two crossed polarizers of polarizing microscope model CENSICO (7626) fitted with a hot stage. Light intensity coming from eyepiece through the sample with the variation of temperature has been measured by a light detector. The 0% and 100% optical transmittance has also been measured for empty and black ink filled sample holder to calculate the percentage optical transmittance.

3. Results and Discussion

Figures 2 and 3 represent typical frequency dependence spectra of the real and imaginary part of the dielectric permittivity measured for $C_4P_Y10B\bar{a}$ and $C_4P_Y12B\bar{a}$. The real part of dielectric permittivity is either constant or decreases with increasing frequency [9]. The observed low value of ε' at higher frequency suggests that the molecule rotates about their molecular axis [10] or some of its side group rotates and gave rise to this kind of absorption.

Figures 4 and 5 show the variation of dielectric loss with respect to frequency for $C_4P_Y10B\bar{a}$ and $C_4P_Y12B\bar{a}$, respectively. Figure 4 shows that the dielectric loss decreases slowly with increase in frequency up to 10 kHz as expected [11–17] and after that the values become constant with further increase in frequency. The dielectric spectrum is hard to interpret because no relaxation peaks are observed between 100 Hz to 10 MHz for both the samples. It may be expected to be due to two possibilities arising in the absorption process. First, the relaxation peak may be occurring below 100 Hz, which is not of molecular origin but due to some ions leading to interfacial polarization as has been reported for some other liquid crystal materials earlier [18] and the second possibility is that the relaxation peak is above

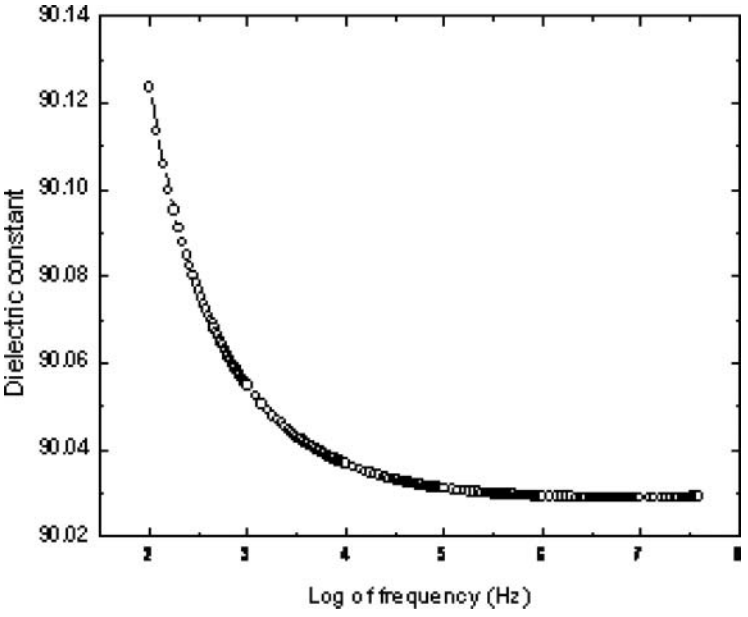

Figure 2. Variation of dielectric permittivity with log of frequency for $C_4P_y10B\bar{a}$.

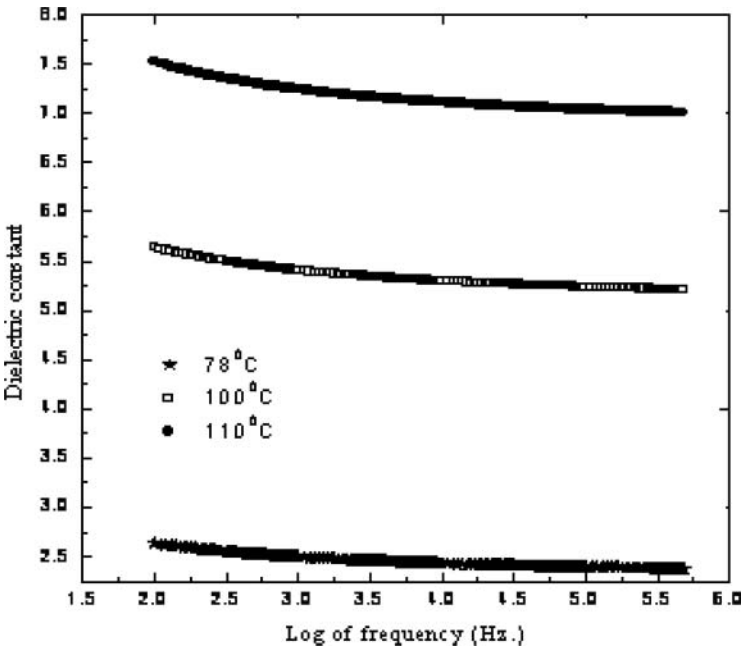

Figure 3. Variation of dielectric permittivity with log of frequency for $C_4P_y12B\bar{a}$.

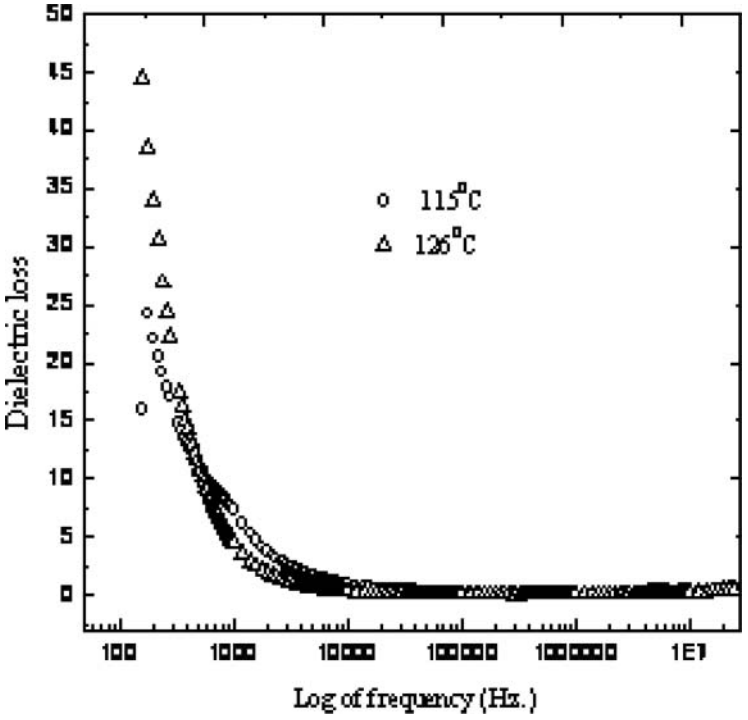

Figure 4. Variation of dielectric loss with log of frequency for $C_4P_y10B\bar{a}$.

10 MHz. It is then assigned to be due to the diffusional reorientation around the long molecular axis [19]. Similar type of behavior has been observed for $C_4P_Y12B\bar{a}$ as is expected.

Figures 6 and 7 show the variation of dielectric permittivity with respect to temperature for $C_4P_Y10B\bar{a}$ and $C_4P_Y12B\bar{a}$, respectively. The variation of dielectric permittivity for each sample is shown during the heating cycle. The values of dielectric permittivity increase with increase in temperature. For each sample dielectric permittivity values show sharp discontinuities clearly indicating the change in phase. This type of behavior has also been reported by other workers for other type of LC samples [20]. On comparing both the figures, it is clear that the values of the dielectric constant are quite high for $C_4P_Y12B\bar{a}$ with respect to $C_4P_Y10B\bar{a}$.

Figures 8 and 9 show the variation of dielectric loss with respect to temperature for $C_4P_Y10B\bar{a}$ and $C_4P_Y12B\bar{a}$, respectively. In Fig. 8, the values of imaginary part of permittivity remain almost constant in temperature range of 30°C to 97°C and its value varies slightly at 100°C showing smectic I to smectic C phase transition of the sample. The figures also show another phase changes at 108°C of smectic C to nematic phase and a sharp increase in permittivity at 123.0°C shows that sample becomes isotropic at this temperature. This type of behavior has also been reported by other groups for other type of liquid crystal sample [21]. A similar behavior has also been observed for $C_4P_Y12B\bar{a}$ as shown in Fig. 9.

3.1 Thermal Microscopy Studies

The hydrogen bonded complex **10OBA-4PyA** exhibits a droplet texture at 121.1°C characterizing the phase as a nematic phase. Further cooling of the sample showed a transition at

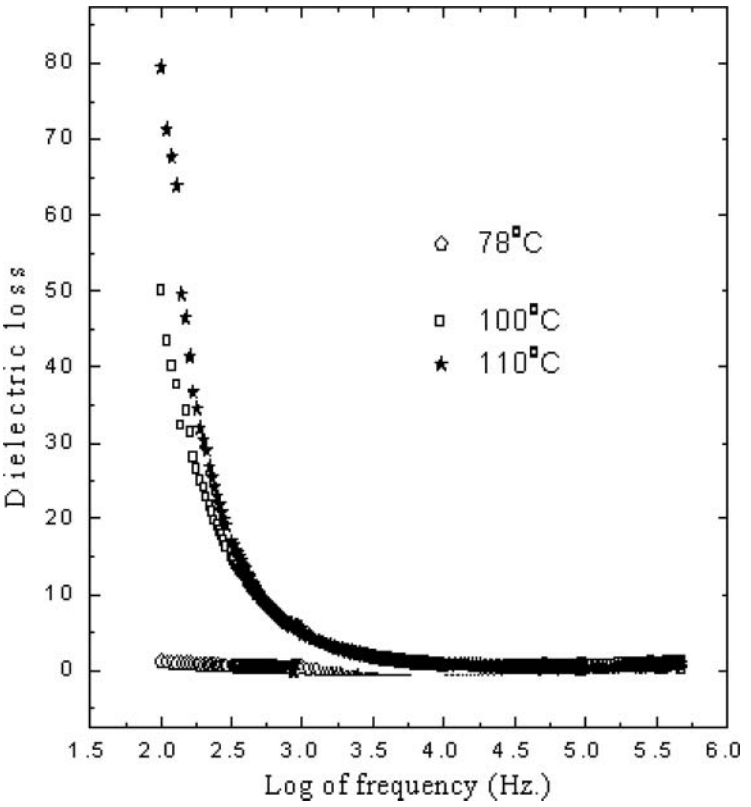

Figure 5. Variation of dielectric loss with log of frequency for $C_4P_y12B\bar{a}$.

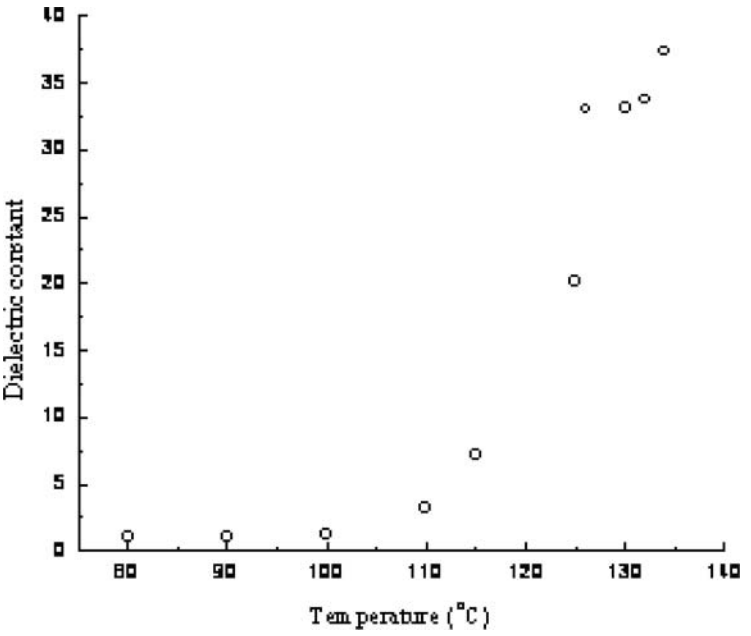

Figure 6. Variation of dielectric permittivity with temperature for $C_4P_y10B\bar{a}$.

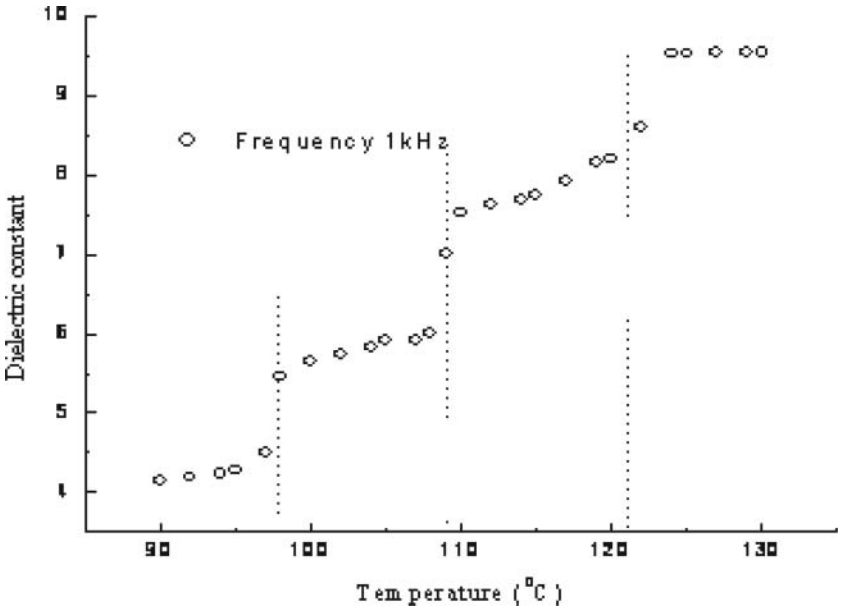

Figure 7. Variation of dielectric permittivity with temperature for $C_4P_y12B\bar{a}$.

108.7°C with a transformation to a Schlieren texture characterizing the phase as a smectic C phase. On further cooling, the sample exhibited a platelet texture at 98.6°C characterizing the phase as a smectic I.

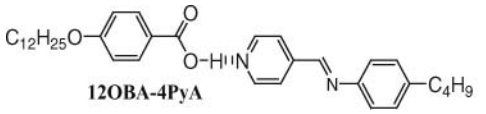

12OBA-4PyA

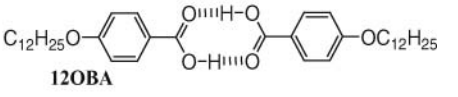

12OBA

Phase transition behavior

$[12OBA]_2$	C	95.2°C	SmC	132.4°C	N	138.7°C	I
[12OBA-4PyA]	SmI	98.5°C	SmC	108.7°C	N	122.8°C	I
4PyA	Room temperature isotropic liquid						

The nematic-isotropic phase transition occurs at 122.9°C in the heating cycle. In the cooling cycle, the hydrogen bonded complex **12OBA-4PyA** exhibits characteristic droplet texture at 122.8°C characterizing the phase as nematic phase. On further cooling cycle, the sample exhibited a Schlieren texture at 108.6°C characterizing the phase as a smectic C. On further cooling, the sample exhibited a characteristic platelet resembling the smectic I phase.

The optical transmittance data as a function of temperature have been plotted for $C_4P_Y10B\bar{a}$ and $C_4P_Y12B\bar{a}$ respectively.

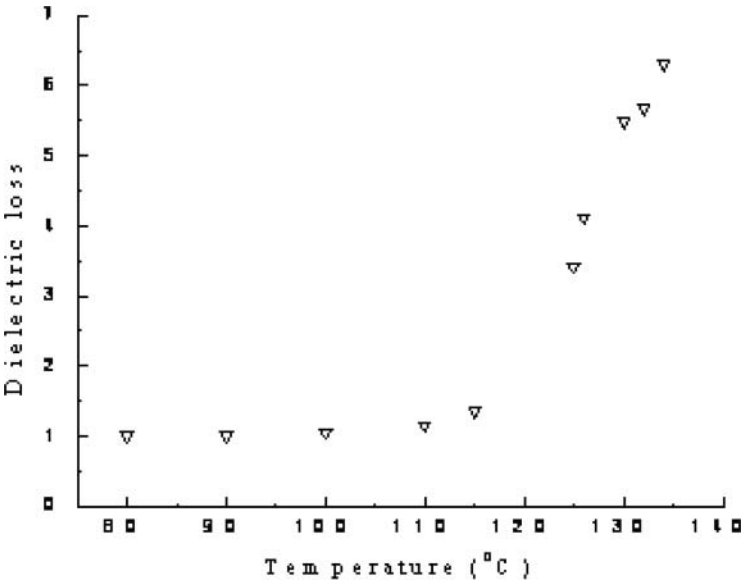

Figure 8. Variation of dielectric loss with temperature for $C_4P_y10B\bar{a}$.

Samples show the following phase sequence as determined by optical transmittance measurement

$$C_4P_Y10B\bar{a} \quad I \xrightarrow{121.1^\circ C} N \xrightarrow{108.5^\circ C} SmC \xrightarrow{96.5^\circ C} SmI$$

$$C_4P_Y12B\bar{a} \quad I \xrightarrow{122.8^\circ C} N \xrightarrow{108.7^\circ C} SmC \xrightarrow{98.6^\circ C} SmI$$

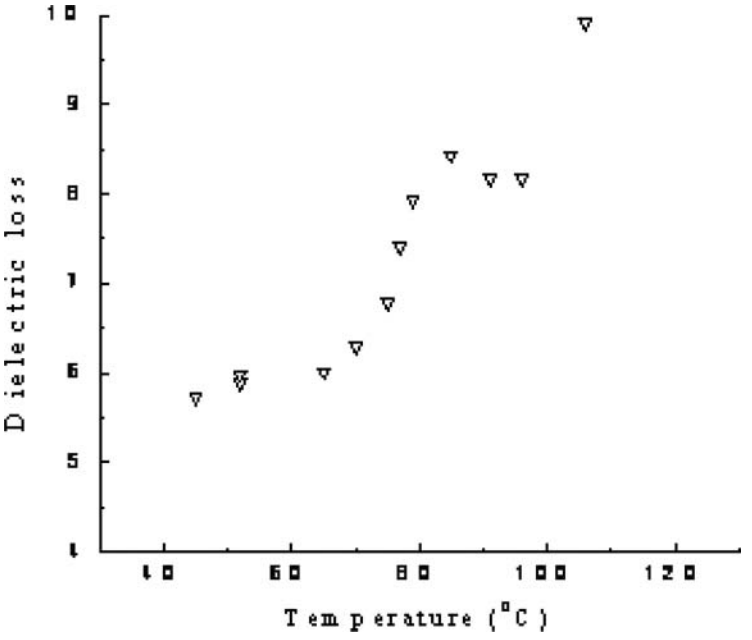

Figure 9. Variation of dielectric loss with temperature for $C_4P_y12B\bar{a}$.

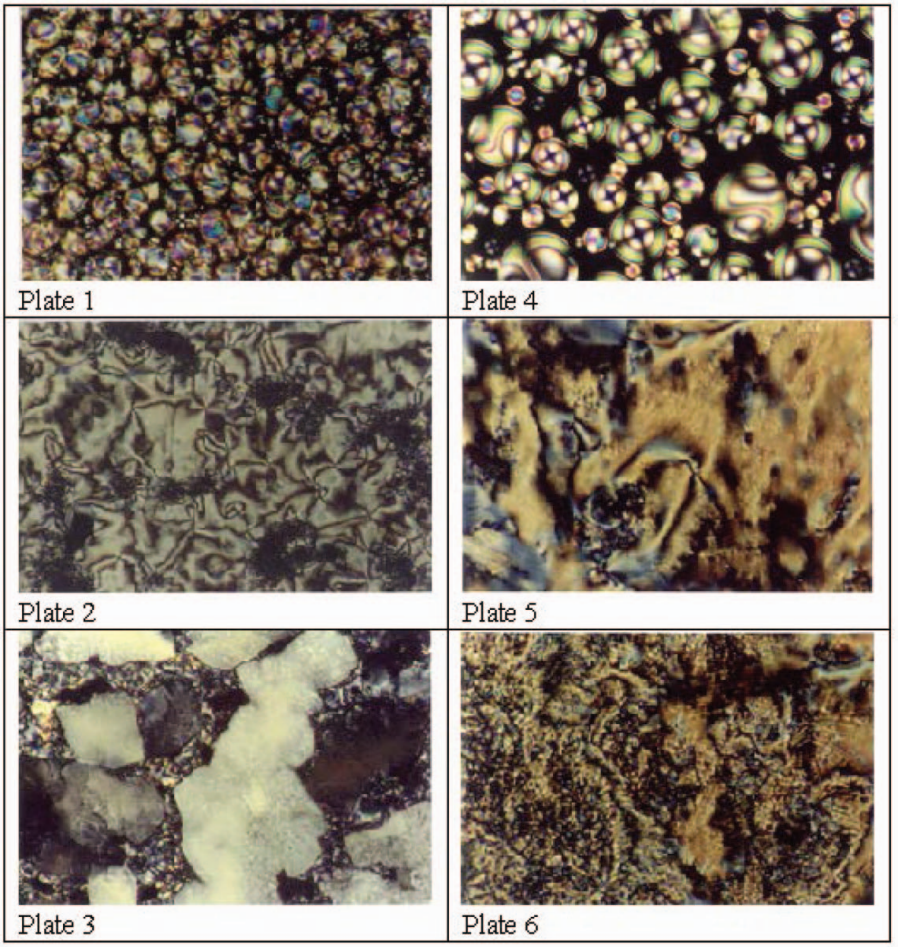

Figure 10. Variation of % optical transmittance with temperature for $C_4P_y10B\bar{a}$

Figures 10 and 11 show the variation of percentage optical transmittance for the samples $C_4P_Y10B\bar{a}$ and $C_4P_Y12B\bar{a}$, respectively. The percentage optical transmittance study of $C_4P_Y10B\bar{a}$ shows a sharp increase at 121.1°C indicating the isotropic nematic phase transition and the percentage optical transmittance at this temperature is 89%. The sample exhibits a phase change at 108.5°C and shows a small but noticeable jump with the values of percentage optical transmittance remains constant. It decreases slowly with further decrease in temperature and shows a noticeable jump at 96.5°C reflecting a smectic C—smectic I phase transition. This type of behavior has also been reported for other liquid crystals from our research group [22] as well as by other researchers [23, 24]. In the case of $C_4P_Y12B\bar{a}$, similar behavior is also observed but the jumps in the transmittance at the phase transitions are noticeable. Further, these studies also supported the observations made by thermal microscopy. The only difference is that the value of percentage optical transmittance for $C_4P_Y10B\bar{a}$ at 100°C is lower than the transmittance observed for $C_4P_Y12B\bar{a}$. This can be interpreted by looking at the fact that the molecules absorb light much strongly.

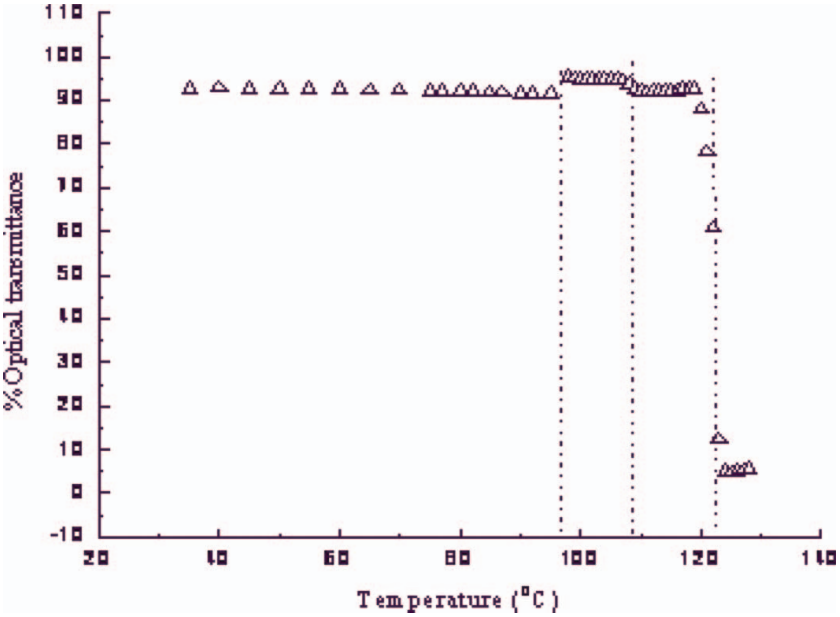

Figure 11. Variation of % optical transmittance with temperature $C_4P_y12B\bar{a}$ (Color figure available online).

4. Conclusions

1. The phase transition study conducted using dielectric and percentage optical transmittance suggest that there is a change in transition temperatures and values of percentage optical transmittance in the two samples explored in the present work due to the presence of a different number of metal ions.
2. The relaxation phenomenon remains undetected as explained in discussion section.
3. For both the samples, the transition temperatures obtained by dielectric and optical techniques are in good agreement with each other.

Acknowledgment

The authors are thankful to DST, ISRO and BRNS UGC for providing grant project no. ISRO/OGP-75.

References

[1] Lehn, J. M. (1985a). *Science*, *227*, 849. Lehn, J. M. (1988b). *Angew. Chem. Int. Ed. Engl*., *27*, 89. Lehn, J. M. (1990c). *Angew. Chem. Int. Ed. Engl*., *29*, 1304.

[2] Kato, T., & Frchet, J. M. J. (1989a). *J. Am. Chem. Soc.*, *111*, 8533. Kato, T., Fujishima, A., & Frechet, J. M. J. (1992b). *Chem. Lett.*, 265. Kato, T., Fujishima A., & Frechet, J. M. J. (1990c). *Chem. Lett.*, 919. Gimeno, N., Ros, M. B., Serrano, J. L., & Fuente, M. R. (2004d). *Angew Chem. Int. Edn.*, *43*, 5235.

[3] Kato, T., Mizoshita, N., & Kishimoto, K. (2006). *Angew Chem. Int. Ed. Engl.*, *45*, 38.

[4] Paleos, C. M., & Tsiourvas, D. (2001). *Liq. Cryst.*, *28*, 1127.

[5] Kato, T. (1998a). In: D. Demus, J. Goodby, G. W. Gray, H. W. Spiess, & V. Vill (Eds.), *Handbook of Liquid Crystals*, Wiley-VCH: Weinheim, pp. 969–979. Blunk, D., Praefcke, K., & Vill, V. In:

D. Demus, J. Goodby, G. W. Gray, H. W. Spiess, & V. Vill (Eds.), *Handbook of Liquid Crystals*, Wiley-VCH: Weinheim, pp. 305–340.
[6] Kato, T. (2002). *Science*, *295*, 2414.
[7] Manohar, R., Tripathi, G., Singh, A. K., Srivastava, A. K., Shukla, J. P., & Prajapati, A. K. (2006). *J. of Phys. and Chem. of Solids*, *67*, 2300–2304.
[8] Singh, A. K., Manohar, R., Shukla, J. P., & Biradar, A. M. (2005). *J. Phys. Chem. Solids*, *66*, 1183.
[9] Viciosa, M. T., Nunes, A. M., Godinho, M. H., & Dionisio, M. D. (2002). *Liq. Cryst.*, *29*(3), 429.
[10] Arora, V. P., & Agarwal, V. K. (1991). *Ind. J. of Pure and Appl. Phys.*, *29*, 769.
[11] Biradar, A. M., Hiller, S., Pikin, S. A., & Hasse, W. (1996). *Liq. Cryst.*, *20*, 247.
[12] Kundu, S. K., Suzuki, K., & Chaudhary, B. K. (2003). *J. Appl. Phys.*, *94*, 2271.
[13] Hiller, S., Biradar, A. M., Wrobel, S., & Hasse, W. (1996). *Phys. Rev. E*, *53*, 641.
[14] Muller, H. J., & Jayaraman, S. (1998). *Mol. Cryst. Liq. Cryst.*, *309*, 93.
[15] Thakur, A. K., Sharma, D. K., Singh, S. P., Bawa, S. S., & Biradar, A. M. (2003). *Ferroelectrics*, *289*, 63.
[16] Dejeu, W. H., & Lathouwers, T. W. (1973). *Mol. Cryst. Liq. Cryst.*, *26*, 225.
[17] Cummins, P. G., Dunmur, D. A., & Laidler, D. A. (1975). *Mol. Cryst. Liq. Cryst.*, *30*, 109.
[18] Biradar, A. M., Kilian, D., Wrobel, S., & Hasse, W. (2000). *Liq. Cryst.*, *27*, 225.
[19] Hasse, W., Wrobel, S., & Falk, K. (2003). *Pramana-Journal of Physics*, *61*(2), 198.
[20] Hohmutha and Schieweb (1981). *Liq. Cryst.*, *22*, 2011.
[21] Agrawal, A., Arora, V. P., Kaushik, V., Anand, P. P., Agrawal, V. K., & Bahadur, B. (1989). *Ind. J. Pure Appl. Phys.*, *27*, 299.
[22] Manohar, R., Gupta, M., & Shukla, J. P. (2004). *J. Phys. and Chem. of Solids*, *61*, 1465.
[23] Shussarenko, S., & Francescangeli, O (1997). *Appl. Phys. lett.*, *71*, 3613.
[24] White, D. L., & Taylor, G. N. (1974). *J. Appl. Phys.*, *45*, 4718.